DOI: 10.17344/acsi.2021.7336 *Acta Chim. Slov.* **2022,** *69,* 448–457

Scientific paper

Optimisation of Amphiphilic-Polymer Coatings for Improved Chemical Stability of $NaYF_4$-based Upconverting Nanoparticles

Tina Černič,[1,2] Monika Koren,[3,4] Boris Majaron,[3,4] Maja Ponikvar-Svet[5] and Darja Lisjak[1,*]

[1] *Jožef Stefan Institute, Department for Materials Synthesis, Ljubljana, Slovenia*

[2] *Jožef Stefan International Postgraduate School, Ljubljana, Slovenia*

[3] *Jožef Stefan Institute, Department of Complex Matter, Ljubljana, Slovenia*

[4] *Faculty of Physics and Mathematics, University of Ljubljana, Slovenia*

[5] *Jožef Stefan Institute, Department of Inorganic Chemistry and Technology, Ljubljana, Slovenia*

** Corresponding author: E-mail: darja.lisjak@ijs.si*
+386 1 4773879

Received: 12-20-2021

Abstract

$NaYF_4$ nanoparticles codoped with Yb^{3+} and Tm^{3+} exhibit upconversion fluorescence in near-infrared and visible spectral range. Consequently, such upconverting nanoparticles (UCNPs) can be used as contrast agents in medical diagnostics and bioassays. However, they are not chemically stable in aqueous dispersions, especially in phosphate solutions. Protective amphiphilic-polymer coatings based on poly(maleic anhydride-*alt*-octadec-1-ene) (PMAO) and bis(hexamethylene)triamine (BHMT) were optimised to improve the chemical stability of UCNPs under simulated physiological conditions. Morphologies of the bare and coated UCNPs was inspected with transmission electron microscopy. All samples showed intense UC fluorescence at ~800 nm, typical for Tm^{3+}. The colloidal stability of aqueous dispersions of bare and coated UCNPs was assessed by dynamic light scattering and measurements of zeta potential. The dissolution of UCNP in phosphate-buffered saline at 37 °C, was assessed potentiometrically by measuring the concentration of the dissolved fluoride. Protection against the dissolution of UCNPs was achieved by PMAO and PMAO crosslinked with BHMT.

Keywords: Nanoparticles; upconversion; dissolution; chemical stability; coatings

1. Introduction

Upconverting nanoparticles (UCNPs) show great potential for various applications in biomedicine as multimodal contrast agents in bioimaging and bioanalysis, nanothermometry, biosensorics and nanotheranostics.[1–4] These applications are based on the UC fluorescence of visible or near-infrared (NIR) light. The sensitising Yb^{3+} ions are excited with NIR light around 980 nm, and the absorbed energy is transferred to the activator Er^{3+}, Yb^{3+} or Ho^{3+} ions emitting light with lower wavelengths.[5] The NIR emission of Tm^{3+} around 808 nm is of particular interest for biomedicine, due to its deeper penetration in biological tissues compared to visible or ultraviolet light. To achieve a high quantum yield of UC fluorescence, fluoride crystalline matrices are preferred to incorporate lanthanide dopants. One of such matrices is β-$NaYF_4$ with hexagonal structure, where Na^+ and Y^{3+} occupy two different sites among the close-packed F^- ions.[6]

The first condition for practical application of any nanoparticles is their chemical and colloidal stability, which strongly depends on their surface chemistry and surrounding medium. Nanoparticles are prone to fast surface reactions, dissolution and severe agglomeration due to their large surface area. Specifically, UCNPs intended for biomedicine must be stable in aqueous media, includ-

ing physiological buffers. The colloidal stability of nanoparticles is achieved by optimising their surface chemistry to induce: (i) electrostatic repulsion by tuning the surface charge or/and (ii) steric repulsion with large molecules (e.g., polymers). The chemical and colloidal stability of nanoparticles becomes more challenging with the increasing complexity of the aqueous media. The primary origin of the colloidal destabilisation of nanoparticles in physiological buffers is high ionic strength that decreases the repulsive electrostatic energy between the nanoparticles, which is otherwise sufficiently high in pure water. Additionaly, the colloidal destabilisation of nanoparticles in complex aqueous media can also be induced by the exchange of the stabilising surface ligands with species having a higher affinity towards the surface metal ions but lower surface charge. Similarly, the dissolution of nanoparticles can be promoted when the exchanging species bond more strongly with the surface ions than the latter are bonded with the crystalline core. For example, the fluoride-based UCNPs dissolve in phosphate solutions (e.g., in phosphate-buffered saline; PBS) due to strong interaction between the surface rare-earth ions and dissolved phosphate ions, thus inducing the coprecipitation of highly stable rare-earth phosphates.[7] Any dissolution of fluoride-based UCNPs *in vivo* can cause various adverse effects[4,8–11] which questions their suitability for applications in biomedicine. The protection of fluoride-based UCNPs against the dissolution and interaction with solutes from the surrounding media is necessary also to ensure stable optical properties. It was shown that even a minor dissolution of the $NaYF_4$-UCNPs deteriorates their UC fluorescence properties,[12–15] limiting their general applicability.

Possible protective coatings against the dissolution of the $NaYF_4$-based UCNPs in aqueous media were studied in the last few years, starting from silica and phosphonates to more complex polymer coatings.[15–21] Most of these coatings decelerated the dissolution of the UCNPs in water or PBS at room temperature. However, only thick microporous silica coating and amphiphilic poly(maleic anhydride-*alt*-octadec-1-ene) crosslinked with bis(hexamethylene)triamine (PMAO-BHMT) coating significantly suppressed the dissolution of $NaYF_4$-UCNPs in PBS at body temperature. Under the same conditions, bare UCNPs almost completely disintegrated.[16,20] Such a high protective efficiency of the thick silica coatings was attributed to the mechanical barrier for the diffusion of aqueous molecules and solute ions to/from the UCNPs surface. Alternatively, the protection of UCNPs by the PMAO-BHMT was attributed to the coating stability, achieved by crosslinking PMAO with BHMT at the UCNPs surfaces.

This study focuses on amphiphilic coatings since they have been recognised as a suitable strategy towards biocompatible inorganic NPs.[22] We hypothesise that a hydrophobic surface layer from an amphiphilic polymer can form an effective diffusion barrier and suppresses the dissolution of UCNPs. We coated Yb^{3+},Tm^{3+}-codoped β-$NaYF_4$ with different surface fractions of amphiphilic PMAO or PMAO additionally crosslinked with BHMT (PMAO-BHMT, Scheme 1). We compared the colloidal and chemical stability of differently coated UCNPs in aqueous media.

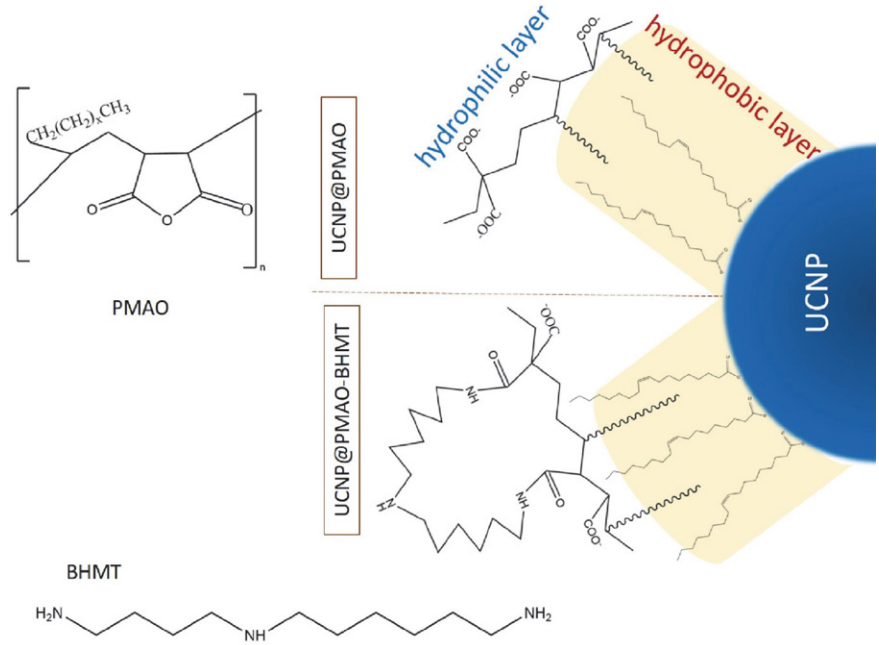

Scheme 1. Chemical formulae of poly(maleic anhydride-*alt*-octadec-1-ene) (PMAO) and bis(hexamethylene)triamine (BHMT) with a schematic presentation of the PMAO (top) and PMAO-BHMT (bottom) coating on an upconverting nanoparticle (UCNP). The inner layer of the coating (yellow) is hydrophobic, while the outer layer is hydrophilic.

2. Experimental

2. 1. Chemicals

Unless otherwise specified, chemicals were used as received. Deionised water was used in all experiments. Ammonium fluoride (98.0%), yttrium(III) chloride hydrate (99.99%), ytterbium(III) chloride hydrate (99.9%), thulium(III) chloride hydrate (99.9%), 1-octadecene (tech. 90%) and oleic acid (tech. 90%) were purchased from Alfa Aesar. The concentration of rare earths in chlorides were determined with an inductively-coupled optical emission spectrometer (ICP-OES, Agilent 720). Poly(maleic anhydride-alt-1-octadecene) (PMAO, Mm 30000–50000), bis(hexamethylene)triamine (BHMT, high purity), sodium hydroxide (≥98%) and chloroform (≥99.8%) were purchased from Sigma Aldrich. Acetone (≥99.8%) and absolute ethanol (≥99.9%) were purchased from Carlo Erba Reagents, while methanol (100%) was purchased from VWR Chemicals. Phosphate-buffered saline (PBS, 10x) was purchased from Alfa Aesar and diluted 10-times before usage to mimic blood's pH and ionic strength.

2. 2. Materials

β-$NaYF_4$ upconverting nanoparticles codoped with Yb^{3+} and Tm^{3+} (named shortly as UCNPs in the subsequent text) with nominal composition $NaY_{0.78}Yb_{0.20}Tm_{0.02}F_4$ were synthesised with a high-temperature coprecipitation, similarly as reported previously.[23,24] In short, lanthanide chlorides (2 mmol) in the stoichiometric ratio were mixed with 12 ml of oleic acid and 30 ml of 1-octadecene in a 100 ml three-neck flask and heated to 156 °C for 30 min. After that, the solution was cooled down to 70 °C, and 10 ml methanol solution of NH_4F (8 mmol) and NaOH (5 mmol) was slowly added. The mixture was stirred for 40 min at 50 °C until methanol evaporated. After that, the solution was heated to 300 °C under an argon atmosphere for 1.5 h. When the reaction solution cooled down to room temperature, acetone was added to sediment the UCNPs. UCNPs were washed several times with ethanol and deionised water, centrifuged (3016 rcf for 5 min), and finally dispersed in chloroform. Three UCNPs batches were distinguished by the average particle diameter (Table 1 and Figure S1 in Supporting Information).

The UCNPs were coated with poly(maleic anhydride-*alt*-octadec-1-ene) (PMAO) and subsequently cross-linked with bis(hexamethylene)triamine (BHMT) by optimising the procedure from Ref.[25]. In short, as-synthesised UCNPs in chloroform were diluted to a concentration of 0.1 mg/ml. The nominal fraction of the PMAO monomer units per UCNPs' surface varied between n = 7–300 MAO/nm^2. First, a chloroform solution of PMAO polymer (100 mg/ml) was admixed to the diluted UCNPs dispersion in a 50-ml flask and stirred for 2 h. Then chloroform solution of BHMT (50 mg/ml) was added with the ratio of 0.5–30 BHMT molecules/nm^2 (i.e., MAO:BHMT = 10:1) and mixed for 30 min. After mixing, chloroform was evaporated using a rotary evaporator. The solid residual was re-dis-

Table 1. Selected samples used in specific comparative studies

Coated polymer	Nominal MAO fraction (no./nm^2)	Sample name UCNPs@...	Average equivalent diameter of the core UCNPs (nm)	Comparative study
PMAO-BHMT	300	PB-*300*	69 ± 3	DLS: Effect of the polymer nominal fraction on the colloidal stability
	105	PB-*105*	52 ± 2	
	20	PB-*20*	52 ± 2	
	7	PB-*7*	52 ± 2	
PMAO	210	P-*210*	52 ± 2	
	105	P-*105*	52 ± 2	
	20	P-*20*	52 ± 2	
	7	P-*7*	52 ± 2	
PMAO-BHMT	150	PB-*150*	69 ± 3	DLS: Long-term colloidal stability (4 months)
PMAO	150	P-*150*	67 ± 5	
PMAO-BHMT	150	PB-*150*	67 ± 5	Chemical stability: dissolution in PBS at physiological conditions
	105	PB-*105*	52 ± 2	
	20	PB-*20*	52 ± 2	
	7	PB-*7*	52 ± 2	
PMAO	150	P-*150*	67 ± 5	
	105	P-*105*	52 ± 2	
	20	P-*20*	52 ± 2	
	7	P-*7*	52 ± 2	

persed in 20 ml of water with 0.5 ml of 1M NaOH and sonicated for 30 min. The dispersion was first filtered with 0.45 μm pore size filters and later centrifuged (15294 rcf for 30 min). The sedimented coated UCNPs were dispersed in deionised water. The samples were labelled as UCNPs@PB-*n*.

An additional set of samples was prepared by coating the UCNPs with PMAO omitting the crosslinking with BHMT. All other parameters were kept the same as above. These samples are labelled as UCNPs@P-*n*.

Firstly, we determined the optimal concentration of as-synthesised UCNPs for the coating procedure, which was 0.1 mg/ml. Secondly, we identified a side reaction when the polymers were used in too large excess. In such a case, the polymers also precipitated homogeneously, not only on the UCNPs surfaces. Therefore, we were lowering the nominal surface density of PMAO from approximately 300 MAO/nm^2 (as in Ref.[25]) down to 7 MAO/nm^2. This optimisation step was done for both types of coatings, UCNPs@PB-*n* and UCNPs@P-*n*. A list of the coated samples used in different comparative studies is given in Table 1.

For comparison, a batch of bare UCNPs was prepared by stripping the surface oleate ligands from the as-synthesised UCNPs. The process was done with a known procedure in conc. HCl.[26]

2. 3. Characterisation

As-synthesised and polymer-coated UCNPs were analysed with a transmission electron microscope (TEM, Jeol 2100). Size distribution of the as-synthesised UCNPs was determined from their surface area as an equivalent diameter using the DigitalMicrograph software (Gatan Inc.). A minimum of 250 particles per sample were accounted for statistics. The crystalline structure of the as-synthesised UCNPs was verified with an X-ray diffractometer (XRD, PANalytical X'Pert pro) using $CuK_{\alpha 1}$ irradiation. The UC fluorescence emission of the UCNPs dispersions was induced with a focused beam from a diode laser emitting 2 W of light at 980 ± 2 nm, and analysed using a compact diffraction spectrometer (Ocean FX Vis-NIR, Ocean Optics) in the 400–900 nm spectral range. Zeta-potential behaviour vs pH was measured in 0.1 mg/ml aqueous dispersions of bare and coated UCNPs with Anton Paar Litesizer^{TM} 500. The pH value was adjusted with 0.1 or 1 M solutions of HCl or NaOH. Hydrodynamic sizes of these aqueous dispersions were measured with dynamic light scattering (DLS, Fritsch, Analysette 12 DynaSizer). The presented results are statistical averages from five measurements with a time interval of 30 s. DLS and zeta potential were also measured in the dispersions of coated UCNPs (0.1 mg/ml) in PBS (both with Litesizer^{TM} 500, Anton Paar).

2. 4. Chemical Stability Studies

Bare and polymer-coated UCNPs were aged under physiological conditions for 3 days. Aqueous dispersions of all samples were filtered beforehand (see Materials Section) to eliminate any potential aggregates that could affect the results. 0.1 mg/ml of bare or coated UCNPs were dispersed in PBS and aged in a thermostatic water bath at 37 °C for 3 days. For comparison, selected samples were also aged at a concentration of 5 μg/ml. After 3 days, the dispersions were cooled to room temperature. The solid fraction was sedimented in a centrifuge (3016 rcf for 5min). For complete removal of the smallest nanoparticles, the supernatant was subsequently ultrafiltered through a 30-kDa membrane. The dissolved fluoride was determined in the filtrates potentiometrically with Orion 960 Autochemistry System, equipped with a temperature sensor and a ion-selective electrode (ISE, Orion 96-09).[27] Three samples were analysed per batch, each one at least in duplicate. For comparison with previous studies, the dissolved fluoride was expressed as the molar fraction of the released fluoride (X_F), calculated by considering the nominal chemical composition of the as-synthesised NPs (Eq. S1 in Supporting Information).

3. Results and Discussion

3. 1. UCNPs with Amphiphilic Polymer Coatings

All as-synthesized UCNPs have the typical shape of hexagonal discs, resulting from their hexagonal crystal structure (Figure 1). Most of the UCNPs lie flat on the sample support, while some are oriented perpendicularly (encircled in Figure 1a), showing that their thickness is approximately one half of their diameter. The UCNPs were relatively homogenous in size; however, the average sizes (i.e., diameters) varied between different synthesis batches (Figure S1 in Supporting Information). Therefore, all direct comparisons were performed on series of samples originating from the same synthesis batch of the UCNPs (Table 1).

TEM investigation revealed the presence of an amorphous layer on the surfaces of all coated UCNPs. The PB coatings appeared thicker than the P coatings (Figure 2). Most of the coated UCNPs were well separated on the TEM-sample support, with a small fraction of (apparent) aggregates of 2–3 UCNPs (Figure S2 in Supporting Information). However, such aggregation may have been induced during the drying of the TEM samples and does not necessarily reflect the situation in the dispersion. In addition, amorphous impurities were observed in the sample coated with the nominal fraction of 300 MAO/nm^2. We assume that the impurities were homogeneously precipitated polymers, since only C and O were identified with EDXS analyses. This was a result of a highly excessive PMAO fraction, in addition to the limited solubility of BHMT in the reaction medium, i.e., chloroform. Therefore, only the samples with ≤150 MAO/nm^2 were used in the subsequent studies.

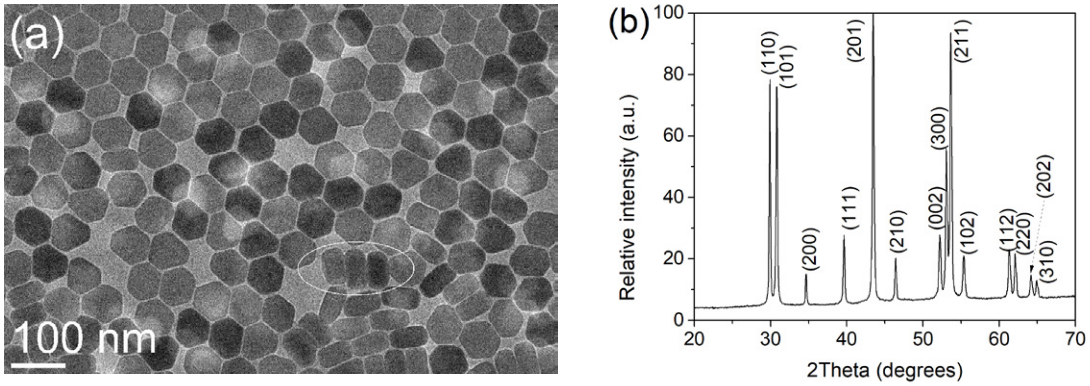

Figure 1. TEM image of the as-synthesised UCNPs (a) and their XRD pattern (b) with indices corresponding to space group $P6_3/m$. Some UCNPs lying perpendicularly to the sample support are encircled in panel (a).

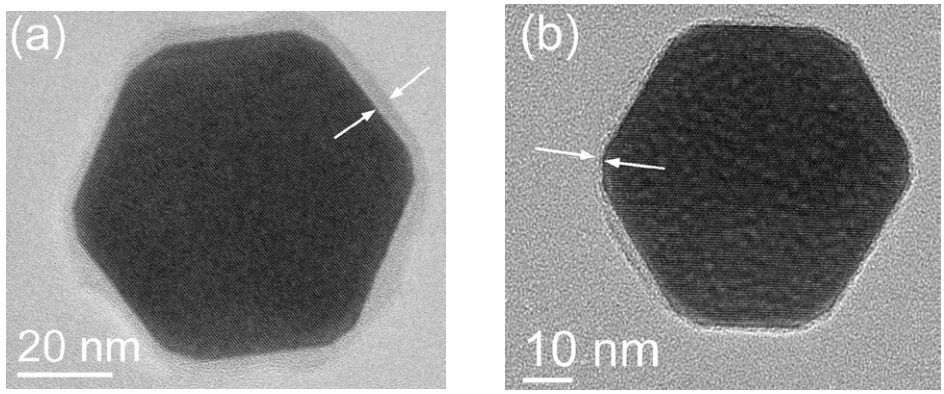

Figure 2. TEM image of a UCNP coated with: @PB-*150* (a) and @P-*150* (b). Arrows point at the amorphous surface layer.

Successful incorporation of Yb^{3+} and Tm^{3+} into the $NaYF_4$ crystal lattice was confirmed by the characteristic UC fluorescence spectra upon excitation at 980 nm, within the strong absorption band of the Yb^{3+} ion (Figure 3). The dominant peak centred at 804 nm corresponds to the transition $^3H_4 \rightarrow {}^3H_6$ of the Tm^{3+} ion, broadened by the Stark splitting of the Tm^{3+} ground-state manifold. The UC fluorescence in the visible region is significantly weaker in comparison. Nevertheless, emission peaks at 452, 477, 648 and 698 nm can be easily identified (see the inset) and assigned to radiative transitions originating from the higher excited levels of the Tm^{3+} ions.

In Figure 3, we can also see a decrease of the UC fluorescence intensities (normalised to the same UCNP mass concentration) upon stripping of the oleate ligands from the as-synthesised UCNPs (dispersed in chloroform) and their transfer to water (bare UCNPs). This is a well-known effect, indicative of the surface quenching by the high-energy vibrations of the water molecules, favouring non-radiative relaxation of the excited levels in Yb^{3+} and Tm^{3+} ions. However, the UC fluorescence spectra of the coated UCNPs in water dispersions demonstrate that both polymer coatings with a high nominal fraction of MAO (*i.e.*, the @PB-*150* and @P-*150*) provide some protection against the surface quenching. In both these cases, the dominant UC emission line (around 800 nm) is ~30% stronger than the bare UCNPs of the same diameter (67 nm).

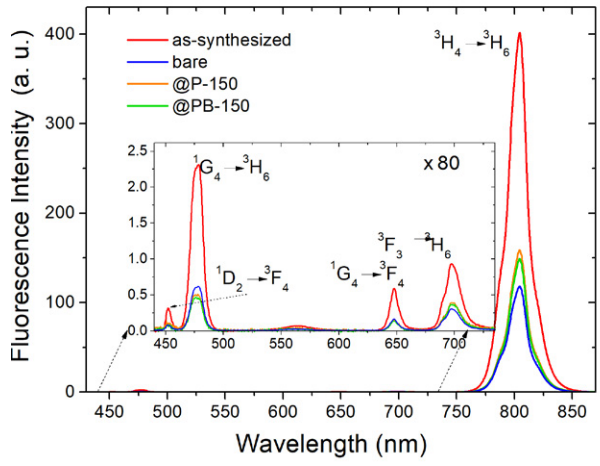

Figure 3. UC fluorescence spectra with the assigned electronic transitions of the as-synthesised oleate-capped UCNPs in chloroform, and bare as well as polymer-coated UCNPs in water. All UCNPs have a core diameter of 67 nm.

The zeta potential of the coated UCNPs is negative at the neutral pH range, and its absolute value decreases with the decreasing pH (Figure 4). This can be explained by deprotonation of surface carboxylic groups, resulting in the negative zeta potential at higher pH values. The carboxylic groups are exposed at the UCNPs surface after the MAO anhydride ring opens in water (Scheme 1). Alternatively, the anhydride ring also opens to react with amine groups of BHMT, and the negative surface-charge density of UCNPs@PB is lower than that of UCNPs@P. The same trend was observed for other nominal fractions. Such zeta-potential behaviour is also an indication that PMAO is crosslinked with BHMT at the UCNPs surfaces, as concluded previously[16] from infrared spectroscopy analysis.

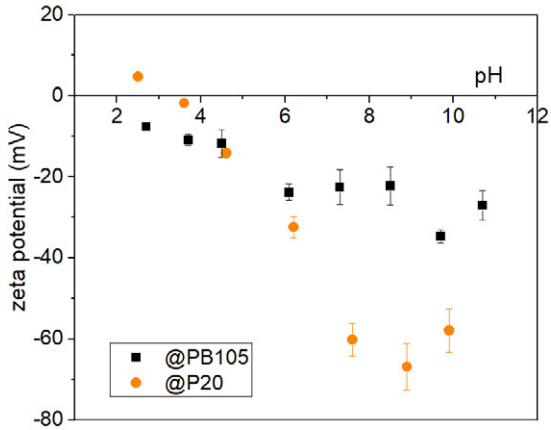

Figure 4. Zeta-potential dependence on pH of the polymer-coated UCNPs.

The colloidal stability of differently coated UCNPs in water was assessed from DLS measurements of the coated UCNPs with an average core diameter of 52 ± 2 nm (Figure 5a and b). The hydrodynamic sizes of the coated UCNPs were, in general, larger than the crystalline core, which can be attributed to the polymer coating and hydration surface layer. The fractions with hydrodynamic sizes ≥ 100 nm indicate some smaller aggregates (Figure S2b in Supporting Information). The absence of larger agglomerates was also in accordance with the transparency of all the dispersions, with the exception of a turbid dispersion of UCNPs@PB-*7* containing some fraction of ~300 nm large NPs. Another exception was the UCNPs@P-*105* dispersion with a small fraction of ~250 nm sized NPs (see the arrow in Figure 5b), suggesting minor aggregation in this sample. In contrast, the dispersion of the UCNPs@PB-*210* contained a significant fraction of ~35 nm sized NPs. These NPs, with the sizes lower than the as-synthesised core UCNPs, were homogeneously precipitated polymer NPs, also identified with TEM and EDXS.

Long-term colloidal stability was examined for the coated UCNPs with 150 MAO/nm^2 within 4 months (Figure 5c). The UCNPs@PB-*150* were, on average, larger than the UCNPs@P-*150*, but the hydrodynamic sizes of both samples were in the range of 1–2 UCNP core sizes (~70 nm) at all times. This demonstrates their long-term stability in water.

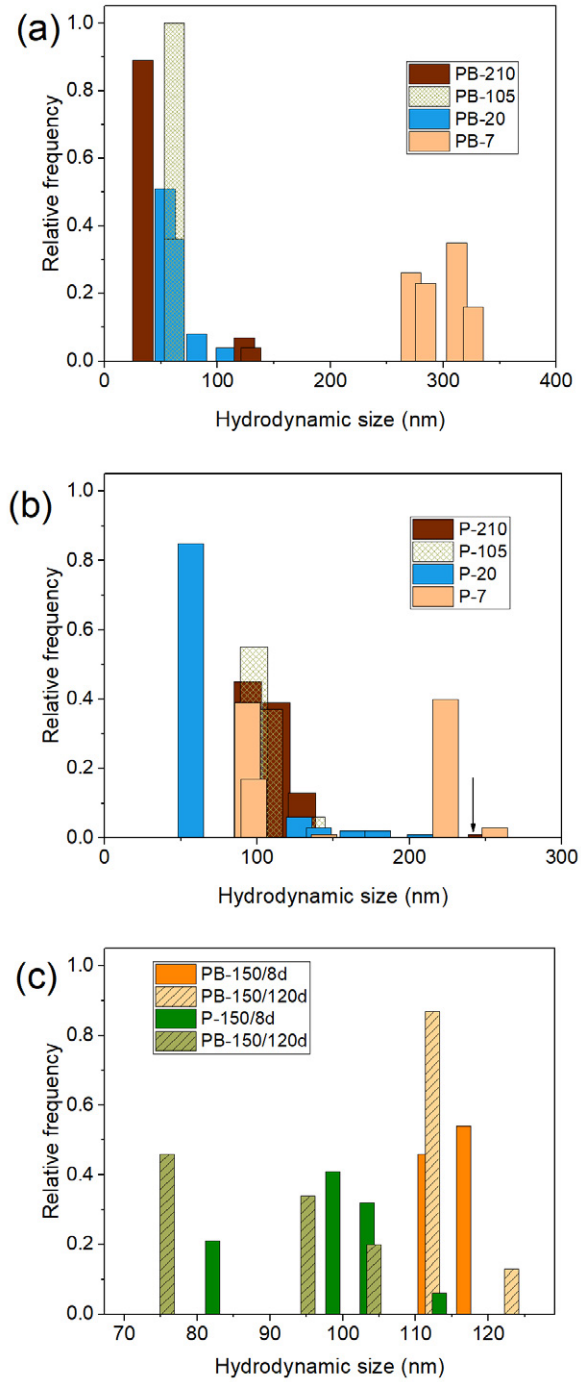

Figure 5. Number-weighted hydrodynamic-size distribution of differently coated UCNPs in water; fresh (a and b) and aged dispersions (c). Core diameters of UCNPs are ~50 nm (a and b), and ~70 nm (c). The arrow in panel (b) points at the very low fraction of the UCNPs@P-*210* at ~250 nm. 8d and 120d in panel (c) denote 8 and 120 days, respectively.

We have also verified the colloidal stability of the coated samples in a physiological buffer, i.e., PBS, used in our chemical-stability studies of the UCNPs. We selected two colloidally stable UCNPs samples in water with the lowest and highest nominal polymer fraction, i.e., UCNPs@P-*20* and UCNPs@PB-*150*. The hydrodynamic size of fresh dispersions of UCNPs@PB-*150* in PBS (Figure 6) was comparable to that in water (Figure 5). However, it increased slightly in 3 days, indicating a slow aggregation of the UCNPs@PB-*150* in PBS, whereas the aggregation of UCNPs@P-*20* in PBS was more significant. After 3 days, a noticeable fraction of aggregates with hydrodynamic sizes of several microns was detected. The colloidal instability can be ascribed to the relatively low absolute value of the zeta potential, i.e., around –10 mV in the fresh PBS dispersions, compared to much higher negative zeta-potential values in water (Figure 4). In addition, the decreasing zeta-potential value with time (>50% in 3 days) indicates some changes in the UCNPs surface chemistry. A TEM inspection of dried PBS dispersions (older than 1 month) did not reveal any significant morphological changes of the coated UCNPs (see example in Figure S3 in Supporting Information). This result demonstrates that the phosphate ions from PBS did not destroy the studied coatings at room temperature. Note that characteristic fibrous decomposition product of bare UCNPs in PBS was observed with TEM even at room temperature,[15] which was not the case in this study. The observed limited colloidal stability of the coated UCNPs in PBS is not critical for their use, since other aqueous media can be used for their storage.

3. 2. Chemical Stability of UCNPs

Our dissolution study represents the most rigorous chemical test of the UCNPs chemical stability under simulated physiological conditions. Namely, the fastest dissolution of UCNPs was so far observed in PBS.[7,12,20] The effect of polymer coatings on the UCNPs dissolution was evaluated by comparing the bare and coated UCNPs aged under the same conditions (Table 2). No significant difference in the X_F-values was observed if the coating was only PMAO or PMAO-BHMT. Both types of polymer coatings almost completely prevented the dissolution of UCNPs. Although differences were not significant, a trend of increasing protecting efficiency in line with the increasing nominal MAO was found. Moreover, no significant difference in the dissolution was found for differently large UCNP, i.e., between ~50 and ~70 nm.

Most of the analysed dispersions contained 0.1 mg/ml of bare or coated UCNPs, which is about the maximum NPs concentration typically used in cytotoxicity and biocompatibility studies (i.e., 1–100 μg/ml).[28–30] It was reported previously that the dissolution of bare UCNPs is more significant for aqueous dispersion with lower concentrations of UCNPs.[12] This was explained with the chemical equilibrium between the dissolved and crystalline fluoride:

$$NaYF_4(s) \overset{H_2O}{\longleftrightarrow} Na^+(aq) + Y^{3+}(aq) + 4F^-(aq) \quad (1)$$

The lower is the concentration of dispersed UCNPs, the larger fraction of UCNPs (i.e., larger X_F) dissolves to reach the equilibrium in Eq. 1. The decomposition mechanism of UCNPs in PBS is not that simple because it is accompanied by the precipitation of Y-phosphates:

$$NaYF_4(s) + PO_4^{3-}(aq) \overset{PBS}{\longleftrightarrow} Na^+(aq) + \\ + YPO_4(s) + 4F^-(aq) \quad (2)$$

Eq. 2 is a simplified equilibrium where we consider only one phosphate form. The concentration of all solutes in PBS (phosphates, NaCl, KCl) is very large and can be considered constant. Therefore, the fraction of dissolved fluoride should also increase with the decreasing UCNPs concentration in PBS as in pure water (Eq. 1). For the verification, we analysed a couple of dispersions containing only 5 μg/ml UCNPs in PBS. Indeed, the X_F-values of the

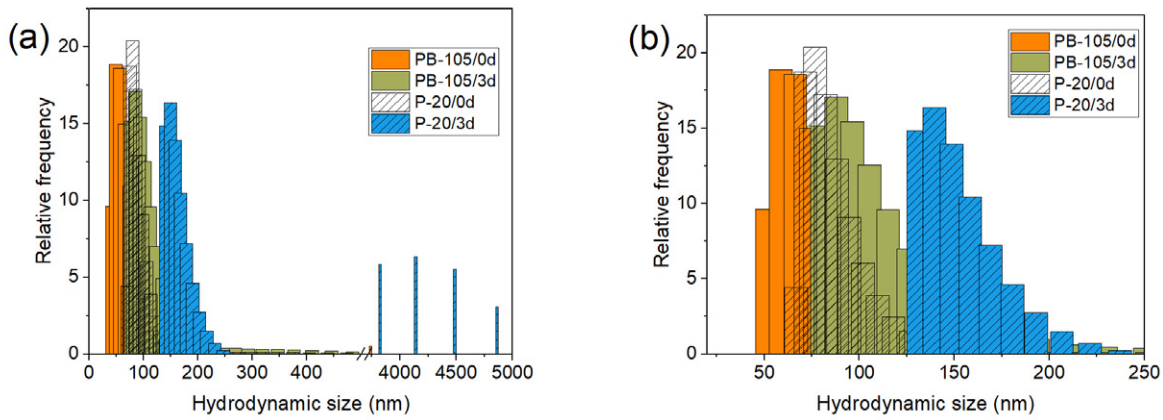

Figure 6. Number-weighted hydrodynamic-size distribution of differently coated UCNPs in PBS; fresh (0d)) and 3-days old dispersions (3d). Core diameters of UCNPs ~ 50 nm. Panel (b) shows an enlarged section of panel (a)

Table 2. Released fluoride concentration after ageing the aqueous dispersions bare or polymer-coated UCNPs (0.1 mg/ml) in PBS at pH 7.4 and 37 °C for 3 days: measured concentration (C_F), molar fraction considering the total solid content (X_F; Eq. S1 in Supporting Information).

Coating	Size of core UCNPs (nm)	C_F (μg/ml)	X_F (mol. %)
none	67 ± 5	30 ± 1	83 ± 4
@PB-*150*	67 ± 5	0.19 ± 0.04	0.52 ± 0.04
@PB-*105*	52 ± 2	<0.1	<0.27
		0.07 ± 0.05*	3.8 ± 2.9*
@PB-*20*	52 ± 2	0.2 ± 0.1	0.6 ± 0.4
@PB-*7*	52 ± 2	0.33 ± 0.05	0.9 ± 0.1
@P-*150*	67 ± 5	0.4 ± 0.1	1.1 ± 0.3
@P-*105*	52 ± 2	<0.1	<0.27
@P-*20*	52 ± 2	0.20 ± 0.01	0.55 ± 0.02
		0.03 ± 0.01*	1.4 ± 0.6*
@P-*7*	52 ± 2	0.15 ± 0.03	0.41 ± 0.08

* dispersions with 5 μg/ml UCNPs

UCNPs@PB-*105* and @P-*20* were larger for lower (5 μg/ml) than for the higher UCNPs concentrations (0.1 mg/ml) (Table 2). This indicates that the hydrophobic surface layer is an efficient barrier to significantly slow down the dissolution of UCNPs, but it does not prevent it completely.

The X_F values of the UCNPs@P and @PB are comparable to those obtained with UCNPs coated with a thick (~70 nm) silica shell and by far lower than with any other protective coatings tested at similar conditions.[15,20,21] This means that our ~1 nm-thick polymer coating with the solvation layer of ≤25 nm (as estimated from the hydrodynamic size) provides for equivalent protection against the dissolution of UCNPs as the 70-nm silica shell.[20]

If the dissolution cannot be completely prevented, it is crucially important for *in vivo* applications to, at least, reduce the dissolution rate to such an extent that the concentration of dissolved species remains insignificant until the UCNPs are excreted from the body. We estimate that 3 days would be the required time for their excretion after being used as contrast agents. The measured concentration of released fluoride (C_F, Table 2) is the fluoride concentration that would interact *in vivo* if the dissolution kinetics is assumed similar to the studied system. The studied polymer coatings suppress the dissolution of UCNPs to such an extent that the released fluoride (≤0.33 μg/ml) would not exceed the acceptable daily intake of fluoride for humans, ADI = 50 μg/kg body mass/day,[11] even if 10 ml of the coated-UCNPs dispersion with a concentration of 0.1 mg/ml would be administered. Altough, we have not found any data on the toxicity of rare earths in humans, a rough estimation was done. If we consider complete dissolution of studied UCNPs as in water (Eq. 1) with the dissolution rate comparable to that in PBS, the released ~0.5 μg/ml of rare-earth ions (Y^{3+}, Yb^{3+} and Tm^{3+}) from 10 ml of dispersion would not exceed the median lethal dose, LD_{50} = 500 mg/kg body mass determined in mice.[31] So, we conclude that the studied polymer coatings, PMAO and PMAO-BHMT, show a promise for safe application of UCNPs in biomedical diagnostics. Moreover, free carboxyl groups of PMAO can be subsequently functionalised for specific *in vivo* applications.

4. Conclusions

We studied amphiphilic-polymer coatings made of poly(maleic anhydride-*alt*-octadec-1-ene) (PMAO) and bis(hexamethylene)triamine (BHMT) to improve the chemical stability of upconverting nanoparticles (UCNPs) based on $NaYF_4$ codoped with Yb^{3+} and Tm^{3+} that decompose in aqueous phosphate solutions. The decomposition of UCNPs was followed by measuring the concentration of released fluoride phosphate-buffered saline (PBS) at physiological conditions. PMAO coating formed directly on the as-synthesised oleate-capped UCNPs. Hydrophobic chains of the amphiphilic PMAO and oleate formed a diffusion barrier for the solutes and solvent molecules. Consequently, the decomposition of the PMAO-coated UCNPs in PBS at physiological conditions was almost completely suppressed. Subsequent crosslinking of PMAO coating with BHMT resulted in a similarly low concentration of the released fluoride, which was for all samples ≤0.33 μg/ml, i.e., well below the acceptable daily intake of fluoride for humans. We conclude that the chemical stability of UCNPs was achieved with the hydrophobic diffusion barrier and that the crosslinking of PMAO with BHMT on the UCNPs surface was not necessary. The PMAO-coated UCNPs can be subsequently bioconjugated to be suitable for diagnostic applications *in vivo*.

Conflicts of Interest: The authors declare no conflict of interest.

Supporting Infromation includes the calculation of the molar fraction of the released fluoride (Eq. S1), size-distribution graph of the as-synthesized UCNPs (Figure S1), TEM images of the coated UCNPs (Figure S2) and of the coated UCNPs after being aged in PBS (Figure S3).

Acknowledgement

The authors acknowledge the financial support from the Slovenian Research Agency (research core funding P2-0089, P1-0192, P1-0045, and P3-0067). We thank Center of Excellence in Nanoscience and Nanotechnology (CENN) for the use of TEM (Jeol 2100).

5. References

1. H. Guo, S. Sun, *Nanoscale* **2012**, *4* (21), 6692–6706. **DOI:**10.1039/c2nr31967e
2. H. H. Gorris, U. Resch-Genger, *Anal. Bioanal. Chem.* **2017**, *409* (25), 5875–5890. **DOI:**10.1007/s00216-017-0482-8
3. F. Vetrone, R. Naccache, A. Zamarrón, A. Juarranz de la Fuente, F. Sanz-Rodríguez, L. Martinez Maestro, E. Martín Rodriguez, D. Jaque, J. García Solé, J. A. Capobianco, *ACS Nano* **2010**, *4* (6), 3254–3258. **DOI:**10.1021/nn100244a
4. B. Del Rosal, D. Jaque, *Methods Appl. Fluoresc.* **2019**, *7* (2), 22001. **DOI:**10.1088/2050-6120/ab029f
5. F. Auzel, *Chem. Rev.* **2004**, *104* (1), 139–174. **DOI:**10.1021/cr020357g
6. F. Wang, Y. Han, C. S. Lim, Y. Lu, J. Wang, J. Xu, H. Chen, C. Zhang, M. Hong, X. Liu, *Nature* **2010**, *463* (7284), 1061–1065. **DOI:**10.1038/nature08777
7. D. Lisjak, O. Plohl, J. Vidmar, B. Majaron, M.; Ponikvar-Svet, *Langmuir* **2016**, *32* (32), 8222–8229. **DOI:**10.1021/acs.langmuir.6b02675
8. A. Gnach, T. Lipinski, A. Bednarkiewicz, J. Rybka, J. A. Capobianco, *Chem. Soc. Rev.* **2015**, *44* (6), 1561–1584. **DOI:**10.1039/C4CS00177J
9. H. Oliveira, A. Bednarkiewicz, A. Falk, E. Fröhlich, D. Lisjak, A. Prina-Mello, S. Resch, C. Schimpel, I. V. Vrček, E. Wysokińska, H. H. Gorris, *Adv. Healthc. Mater.* **2019**, *8* (1), 1801233. **DOI:**10.1002/adhm.201801233
10. N. I. Agalakova, G. P.; Gusev, *ISRN Cell Biol.* **2012**, *2012*, 403835. **DOI:**10.5402/2012/403835
11. J. Han, L. Kiss, H. Mei, A. M. Remete, M. Ponikvar-Svet, D. M. Sedgwick, R. Roman, S. Fustero, H. Moriwaki, V. A. Soloshonok, *Chem. Rev.* **2021**, *121* (8), 4678–4742. **DOI:**10.1021/acs.chemrev.0c01263
12. S. Lahtinen, A. Lyytikäinen, H. Päkkilä, E. Hömppi, N. Perälä, M. Lastusaari, T. Soukka, *J. Phys. Chem. C* **2017**, *121* (1), 656–665. **DOI:**10.1021/acs.jpcc.6b09301
13. O. Plohl, M. Kraft, J. Kovač, B. Belec, M. Ponikvar-Svet, C. Würth, D. Lisjak, U. Resch-Genger, *Langmuir* **2017**, *33* (2), 553–560. **DOI:**10.1021/acs.langmuir.6b03907
14. A. Sedlmeier, H. H.; Gorris, H. H. *Chem. Soc. Rev.* **2015**, *44*, 1526–1560. **DOI:**10.1039/C4CS00186A
15. E. Andresen, C. Würth, C. Prinz, M. Michaelis, U. Resch-Genger,. *Nanoscale* **2020**, *12* (23), 12589–12601. **DOI:**10.1039/D0NR02931A
16. O. Plohl, S. Kralj, B.; Majaron, E.; Fröhlich, M.; Ponikvar-Svet, D.; Makovec, D.; Lisjak, *Dalt. Trans.* **2017**, *46* (21), 6975–6984. **DOI:**10.1039/C7DT00529F
17. N. Estebanez, M. González-Béjar, J. Pérez-Prieto, *ACS Omega* **2019**, *4* (2), 3012–3019. **DOI:**10.1021/acsomega.8b03015
18. E. Palo, M.; Salomäki, M.; Lastusaari, *J. Colloid Interface Sci.* **2019**, *538*, 320–326. **DOI:**10.1016/j.jcis.2018.11.094
19. E. Palo, H.; Zhang, M.; Lastusaari, M.; Salomäki, *ACS Appl. Nano Mater.* **2020**. **DOI:**10.1021/acsanm.0c01245
20. M. I. Saleh, B. Rühle, S. Wang, J. Radnik, Y. You, U. Resch-Genger, *Sci. Rep.* **2020**, *10* (1), 19318. **DOI:**10.1038/s41598-020-76116-z
21. M. Vozlič, T. Černič, S. Gyergyek, B. Majaron, M. Ponikvar-Svet, U. Kostiv, D. Horak, D. Lisjak, *Dalt. Trans.* **2021**, *50*, 6588–6597. **DOI:**10.1039/D1DT00304F
22. G. Palui, F. Aldeek, W. Wang, H. Mattoussi, *Chem. Soc. Rev.* **2015**, *44* (1), 193–227. **DOI:**10.1039/C4CS00124A
23. H.-S. Qian,.Y. Zhang, *Langmuir* **2008**, *24* (21), 12123–12125. **DOI:**10.1021/la802343f
24. E. Palo, M. Tuomisto, I. Hyppänen, H. C. Swart, J. Hölsä, T. Soukka, M. Lastusaari, *J. Lumin.* **2017**, *185*, 125–131. **DOI:**10.1016/j.jlumin.2016.12.051
25. G. Jiang, J. Pichaandi,N. J. J. Johnson, R. D. Burke, F. C. J. M. van Veggel, *Langmuir* **2012**, *28* (6), 3239–3247. **DOI:**10.1021/la204020m
26. N. Bogdan, F. Vetrone, G. A. Ozin, J. A. Capobianco, *Nano Lett.* **2011**, *11* (2), 835–840. **DOI:**10.1021/nl1041929
27. D. Štepec, G. Tavčar, M. Ponikvar-Svet, *Environ. Pollut.* **2019**, *248*, 958–964. **DOI:**10.1016/j.envpol.2019.02.046
28. E. Wysokińska, J. Cichos, E. Zioło, A. Bednarkiewicz, L. Strzadała, M. Karbowiak, D. Hreniak, W. Kałas, *Toxicol. Vitr.* **2016**, *32*, 16–25. **DOI:**10.1016/j.tiv.2015.11.021
29. R. Li, Z. Ji, J. Dong, C. H. Chang, X. Wang, B. Sun, M. Wang, Y.-P. Liao, J. I. Zink, A. E. Nel, T. Xia, *ACS Nano* **2015**, No. 3, 3293–3306. **DOI:**10.1021/acsnano.5b00439
30. B. Pem, D. González-Mancebo, M. Moros, M. Oca a, A. I. Becerro, I. Pavičić, A. Selmani, M. Babič, D. Horák, I. Vinković Vrček, *Methods Appl. Fluoresc.* **2019**, *7* (1). **DOI:**10.1088/2050-6120/aae9c8
31. S. Hirano, K. T. Suzuki, *Environ. Health Perspect.* **1996**, *104* (suppl 1), 85–95. **DOI:**10.1289/ehp.96104s185

Povzetek

Nanodelci $NaYF_4$, sočasno dopirani z Yb^{3+} in Tm^{3+}, izkazujejo fluorescenco z energijsko pretvorbo navzgor v bližnjem infrardečem in vidnem spektru. Tovrstne nanodelce z energijsko pretvorbo navzgor (NDEPN) lahko uporabljamo kot kontrastna sredstva v medicinski diagnostiki in bioloških testih. Pomanjkljivost NDEPN je omejena kemijska stabilnost v vodnih disperzijah, še posebej v fosfatnih raztopinah. Optimizirali smo zaščitne amfifilne polimerne prevleke na osnovi poli(maleinski anhidrid-*alt*-oktadec-1-en) (PMAO) in bis(heksametilen)triamin (BHMT) za izboljšavo kemijske stabilnost NDEPN pri simuliranih fizioloških pogojih. Morfologijo izhodnih in prevlečenih NDEPN smo analizirali s presevno elektronsko mikroskopijo. V vseh vzorcih smo izmerili intenzivno fluorescenco pri ~800 nm, značilno za Tm^{3+}. Koloidno stabilnost vodnih disperzij izhodnih in prevlečenih NDEPN smo ocenili z meritvami dinamičnega sipanja svetlobe in zeta potenciala. Raztapljanje NDEPN pri 37 °C v fosfatnem fiziološkem pufru smo spremljali s potenciometričnimi meritvami koncentracije raztopljenega fluorida. Ugotovili smo, da NDEPN lahko pred raztapljanjem zaščitimo s PMAO in s PMAO zamreženim z BHMT.